Resonance Raman Characterization of Reaction Centers with an Asp Residue near the Photoactive Bacteriopheophytin†

Agnes Cua,‡ Christine Kirmaier,§ Dewey Holten,§ and David F. Bocian*,‡

Department of Chemistry, University of California, Riverside, California 92521, and Department of Chemistry, Washington University in St. Louis, St. Louis, Missouri 63130

Received September 29, 1997; Revised Manuscript Received March 2, 1998

ABSTRACT: Q_y-excitation resonance Raman (RR) studies are reported for a series of *Rhodobacter capsulatus* reaction centers (RCs) containing mutations at L-polypeptide residue 121 near the photoactive bacteriopheophytin (BPh_L). The studies focus on the electronic/structural perturbations of BPh_L induced by replacing the native Phe with an Asp residue. Earlier work has shown that the electron-transfer properties of F(L121)D RCs are closely related to those of RCs in which BPh_L is replaced by bacteriochlorophyll (BChl) (beta-type RCs) or by pheophytin. In addition to the F(L121)D single mutant, RR studies were performed on the F(L121)D/E(L104)L double mutant, which additionally removes the hydrogen bond between BPh_L and the native Glu L104 residue. The vibrational signatures of BPh_L in the single and double mutants containing Asp L121 are compared with one another and with those of BPh_L in both wild-type and F(L121)L RCs. The replacement of the aromatic Phe residue with Leu has no discernible effect on the vibrational properties of BPh_L, a finding in concert with the previously reported absence of an effect of the mutation on the electron-transfer characteristics of the RC. In contrast, replacement of Phe with Asp significantly perturbs the vibrational characteristics of BPh_L, and in a manner most consistent with Asp L121 being deprotonated and negatively charged. The negative charge of the carboxyl group of Asp L121 interacts with the π-electron system of BPh_L in a relatively nonspecific fashion, diminishing the contribution of charge-separated resonance forms of the C_9-keto group to the electronic structure of the cofactor. The presence of a negative charge near BPh_L is consistent with the known photochemistry of F(L121)D RCs, which indicates that the free energy of $P^+BPh_L^-$ is substantially higher than in wild-type RCs.

The reaction center (RC)[1] is a membrane-bound protein responsible for the initial charge-separation process in photosynthesis (*1*−*3*). Purple bacterial RCs consist of four bacteriochlorophylls (BChls), two bacteriopheophytins (BPhs), two quinones (Q), a non-heme iron, and a carotenoid arranged in three polypeptide subunits designated L, M, and H. Two of the BChl molecules form a dimer (P). The X-ray crystal structures of RCs from two purple bacteria (*Rhodobacter sphaeroides* and *Rhodopseudomonas viridis*) reveal that P, the accessory BChls, and the BPhs are arranged in the L and M subunits such that the macroscopic symmetry is approximately C_2 (*4*−*7*). Upon excitation, P is elevated to its excited singlet state (P*), which transfers an electron in about 3 ps to the BPh molecule associated with the L polypeptide (BPh_L). This process utilizes the BChl cofactor on the L branch ($BChl_L$) as either a discrete intermediate or a superexchange mediator, or both. Subsequently, BPh_L^- transfers an electron in about 200 ps to its neighboring quinone (Q_A). The quantum yield of the overall process is approximately unity.

The relative free energies of P*, $P^+BChl_L^-$, and $P^+BPh_L^-$ are criticial in determining the rates and yields of both the formation and the decay pathways of $P^+BPh_L^-$, as exemplified by studies of RCs in which BPh_L is replaced by another pigment. Beta-type mutant RCs constitute one general class in this genre (*8*−*12*). In these RCs, a histidine residue is introduced over one face of BPh_L, which results in incorporation of a BChl (designated β) in place of BPh_L. Chemical substitution of BPh_L has also been accomplished with several different tetrapyrroles (*13*−*16*). In both the beta-type and the chemically modified RCs, P* decays with a somewhat longer lifetime than in wild-type RCs to give a P^+I^- transient from which electron transfer to Q_A proceeds with a diminished overall yield of $P^+Q_A^-$. The diminished yield is ascribed to increased involvement of $P^+BChl_L^-$ in state P^+I^-, which facilitates competitive charge recombination to the ground state. The increased involvement of $P^+BChl_L^-$ in beta-type RCs arises because $P^+\beta^-$ is at a higher free energy than $P^+BPh_L^-$, owing to the more negative reduction potential of BChl versus BPh (*17*). [The same arguments apply to the chemically modified RCs (*13*)].

† This work was supported by Grant GM-39781 (D.F.B.) from the National Institute of General Medical Sciences and Grant MCB-9723008 from the National Science Foundation (C.K. and D.H.).

‡ University of California.

§ Washington University in St. Louis.

[1] Abbreviations: BChl, bacteriochlorophyll; BPh, bacteriopheophytin; FT-IR, Fourier transform infrared; L, M, and H, light, medium, and heavy polypeptides of the reaction center; P, the special pair primary electron donor; Q, quinone; RC(s), reaction center(s); RR, resonance Raman; SERDS, shifted-excitation Raman difference spectroscopy.

S0006-2960(97)02410-0 CCC: $15.00
Published on Web 04/18/1998

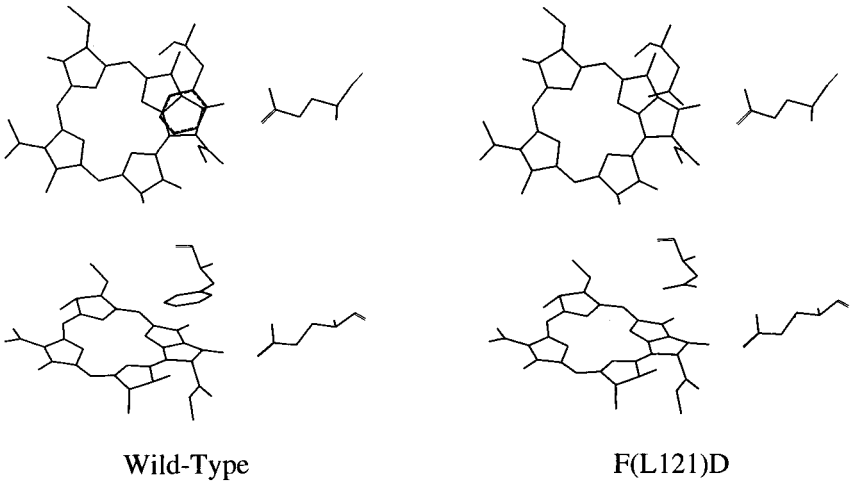

FIGURE 1: Two views of BPh_L showing the locations of residues Phe L121 and Glu L104 in wild-type RCs (left panel), and two views of BPh_L with an Asp residue substituted at position L121 (right panel). In these latter views, the Asp has been positioned by simple replacement of the native Phe residue in the crystal structure. In both views, the phytyl substituent of BPh_L has been removed for clarity. The figure was constructed using the X-ray crystallographic data for *Rps. viridis* RCs (*5*) because X-ray data is not available for *Rb. capsulatus* RCs.

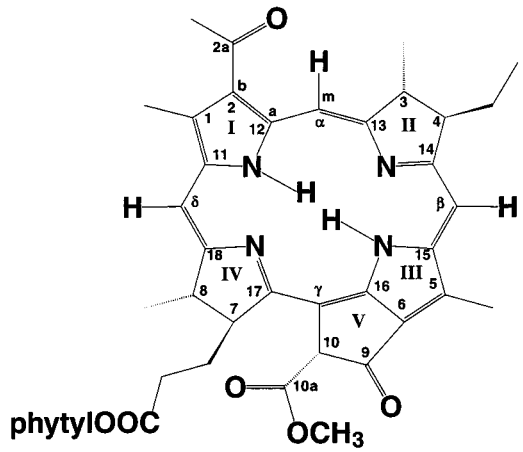

FIGURE 2: Structure and labeling scheme for BPh.

Consequently, P^+I^- is thought to be best characterized as a thermal/quantum admixture of $P^+BChl_L^-$ and $P^+\beta^-$ (*11*, *12*).

Recently, it has shown that beta-type photochemistry can be induced in RCs that retain a normal pigment composition (*18*). This striking change in the primary electron-transfer process was achieved in *Rhodobacter capsulatus* RCs by replacing the native Phe residue at position L121 with an Asp residue. The plane of the aromatic ring of F(L121) is nearly parallel to, and ~3.7 Å away from, ring V of BPh_L (*4*−*7*), as is illustrated schematically in Figure 1 (left panel). Simple substitution of an Asp residue into the crystal structure coordinates of the RC yields a distance of closest approach between Asp L121 and BPh_L of ~3.5 Å, as is illustrated schematically in Figure 1 (right panel). The detailed structure of BPh is shown in Figure 2. The electron-transfer characteristics of F(L121)D RCs indicate that the free energy of $P^+BPh_L^-$ is increased substantially (up to ~175 meV) relative to that of $P^+BPh_L^-$ in wild-type RCs (*18*). This shift is only slightly less than the free-energy increase achieved by replacing BPh_L with β ($P^+\beta^-$ is ~200 meV above $P^+BPh_L^-$ in wild-type RCs (*11*,*18*)), and significantly larger than the redox changes that have been elicited by adding or removing single hydrogen bonds (~60 meV) from a chromophore (*11*, *19*, *20*). Along similar lines, the introduction of an Asp mutation near $BChl_L$ in beta-type RCs, giving the G(M201)D/L(M212)H double mutant, has been shown to raise the free energy of $P^+BChl_L^-$ to such an extent that a low (~15%) yield of electron transfer down the normally inactive M branch of the RC is observed (*12*).

The mechanism by which the Asp residue raises the free energy of the charge-separated intermediate in F(L121)D [or G(M201)D/L(M212)H] RCs is not yet clear. Either the protonated (neutral) or deprotonated (negatively charged) forms of an Asp at L121 would be expected to alter the electronic/redox properties of BPh_L, although the charged residue would have a more substantial effect. These points are borne out by studies of myoglobin in which a charged (e.g., Asp) or neutral (e.g., Asn) residue is placed over the face of the heme cofactor (*21*). The electronic effects of Asp on BPh_L may also have ancillary structural consequences. Alternatively, the Asp mutation could have steric effects on the structure and properties of BPh_L. The existing static and transient optical spectra available for F(L121)D RCs are not sufficient to distinguish between these possibilities. Resonance Raman (RR) spectroscopy provides an attractive means of addressing this issue. The vibrational characteristics of the ring-skeletal and carbonyl modes of BPh_L are sensitive to the interactions between the carbonyl groups of this cofactor and nearby amino acid residues (*22*−*25*). The magnitude and nature of these interactions are in turn governed by the physicochemical properties of the amino acid side chains and their spatial relationship to the chromophore.

In this study, we report RR studies of *Rb. capsulatus* RCs with mutations at position L121, focusing on the vibrational characteristics of the BPh_L cofactor. The RCs examined include the F(L121)D and F(L121)L single mutants and the F(L121)D/E(L104)L double mutant. In the double mutant, the Glu L104 residue, which is known to form a hydrogen bond with the C_9-keto group of BPh_L in wild-type RCs (*4*−*7*, *11*, *19*, *23*−*25*), is replaced with a non-hydrogen-bonding Leu residue. The F(L121)L mutant, which has the same electron-transfer properties as wild-type RCs (*9*), provides a reference sample in addition to wild-type RCs to gauge the effects of the F(L121)D mutation on the vibrational characteristics of BPh_L. All of the RR data were acquired

using excitation into the red-most Q_y absorption bands of the BPh cofactors. Q_y-excitation (as opposed to Q_x- or B-excitation) was chosen both to facilitate RR enhancement of the vibrations of the BPhs over those of the BChls and P and to maximize enhancement of the keto modes of the chromophores (*25*−*33)*. Q_y-excitation maximizes enhancement of the keto vibrations because these groups lie along the *y*-axis of the macrocycle. Collectively, the RR data provide further insights into the effects of the Asp L121 residue on the structural and electronic properties of BPh_L and the protonation/charge state of the Asp residue.

MATERIALS AND METHODS

The *Rb. capsulatus* wild-type, F(L121)L, F(L121)D, and F(L121)D/E(L104)L RCs were prepared, isolated, and purified as previously described (*9*, *18*). The RCs were solubilized in 15 mM Tris-HCl (pH 8)/0.015% Triton X-100. All RCs were Q-reduced by adding a slight excess of a buffered sodium dithionite solution to the sample.

The RR measurements were made at 26 K on optically dense (OD ∼1.0/mm at 800 nm; RC concentration ∼35 μM) snowy samples contained in 1 mm i.d. capillary tubes. The advantages and disadvantages of using snowy versus glassy samples have been previously discussed (*27*). Temperature control was achieved by mounting the sample on a cold tip of a closed-cycle refrigeration system (ADP Cryogenics, DE-202 Displex).

The RR spectra were obtained using a red-optimized triple spectrograph and detection system that has been previously described (*26*). A Ti:sapphire laser (Coherent 890) pumped by an Ar ion laser (Coherent Innova 400-15UV) served as the excitation source. The laser powers were typically 1.0−1.5 mW. The power density on the sample was adjusted by defocusing the incident laser beam. The resulting photon fluxes (∼100 photons s^{-1} RC^{-1}) were low enough that in steady state only a few percent of the RCs existed in photogenerated transient states. Each RR data set was obtained with 3−4 h of signal averaging. The data acquisition time for an individual scan was dictated by the level of background fluorescence from a particular sample (vide infra). These times ranged from 20 to 50 s for the different RCs. Cosmic spikes in the individual scans were removed prior to coaddition of the scans. The spectral resolution was ∼2 cm^{-1} in all spectral regions. The spectral data were calibrated using the known frequencies of fenchone (*34*).

The Q_y-excitation RR spectra for all four RCs were superimposed on an emission background. The fluorescence background was particularly large in the region of the high-frequency ring-skeletal and carbonyl modes (1600−1760 cm^{-1}) which are the principal focus of this study. The fluorescence background, in conjunction with the fact that the Q_y-excitation RR intensity enhancements of the high-frequency modes of BPh are generally weak (*26*, *33*), compromises the quality of the spectra. Therefore, all the RR spectra were acquired using the shifted-excitation Raman difference spectroscopic (SERDS) technique (*31*, *35*). The application of the SERDS method to RCs has been previously described in detail (*27*−*33*). Briefly, each data set is acquired at two excitation wavelengths that differ by a small wavenumber increment (typically 10 cm^{-1}). [The 3−4 h data acquisition time indicated above is for each of the two data sets required to construct a given SERDS trace.] These data sets are subtracted to yield a background-free RR difference (SERDS) spectrum. The RR spectra presented herein were obtained by subtracting the initial spectrum from the shifted spectrum. The spectral window is defined by the initial spectrum and corresponds to the wavenumber axis in the figures. The normal RR spectrum is then reconstructed from the SERDS data by fitting the latter to a series of derivative-shaped functions (in this case, difference bands generated from Gaussian functions) of arbitrary frequency, amplitude, and width. The frequencies marked in the figures correspond to the positions of the bands used in the fits and, thus, do not necessarily correspond to the peak maxima for overlapping bands. In addition, certain bands are marked which are not clearly resolved in the spectra. These bands are indicated because their inclusion noticeably improved the quality of the fits to the SERDS data.

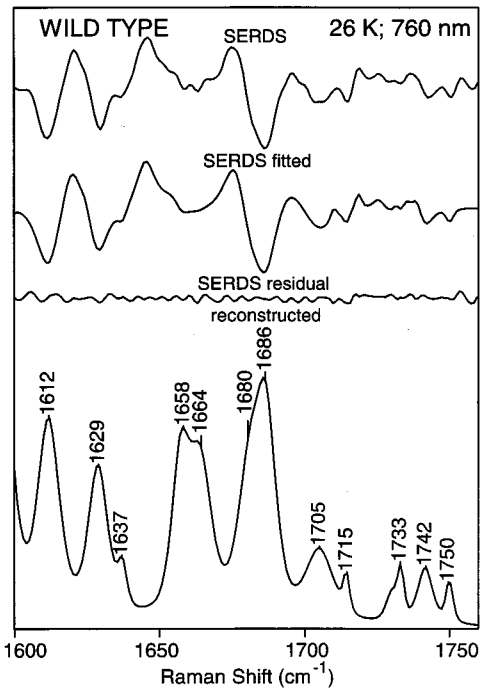

FIGURE 3: Q_y-excitation (λ_{ex} = 760 nm) RR spectrum of the BPhs of wild-type RCs in the region of the carbonyl and high-frequency ring-skeletal modes. The top trace is the raw SERDS data, the second trace is the fit of the SERDS data, the third trace is the SERDS residual (observed − fit), and the bottom trace is the RR spectrum reconstructed from the SERDS data.

RESULTS

The high-frequency regions (1600−1760 cm^{-1}) of the Q_y-excitation (λ_{ex} = 760 nm) RR spectra of *Rb. capsulatus* wild-type and F(L121)D RCs are shown in Figures 3 and 4, respectively. Although the full data acquisition spanned 1300−1760 cm^{-1}, only the highest-frequency region is shown because it exhibits the key spectral differences among the various RCs (vide infra). In both Figures 3 and 4, the top trace is the raw (unsmoothed) SERDS data, the second trace is the fit of the SERDS data, the third trace is the SERDS residual (observed minus fit), and the bottom trace is the RR spectrum reconstructed from the SERDS data. The relatively small residuals compared with the SERDS intensities are indicative of the excellent fidelity of the fits. Comparable signal-to-noise characteristics and SERDS re-

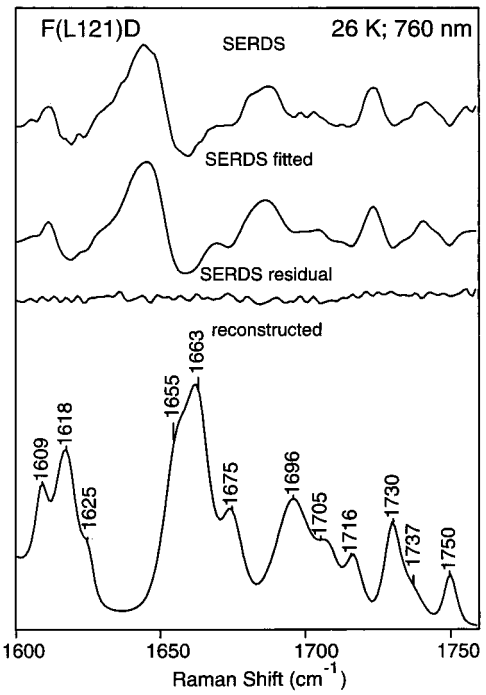

FIGURE 4: Q_y-excitation (λ_{ex} = 760 nm) RR spectrum of the BPhs of F(L121)D RCs in the region of the carbonyl and high-frequency ring-skeletal modes. The top trace is the raw SERDS data, the second trace is the fit of the SERDS data; the third trace is the SERDS residual (observed − fit), and the bottom trace is the RR spectrum reconstructed from the SERDS data.

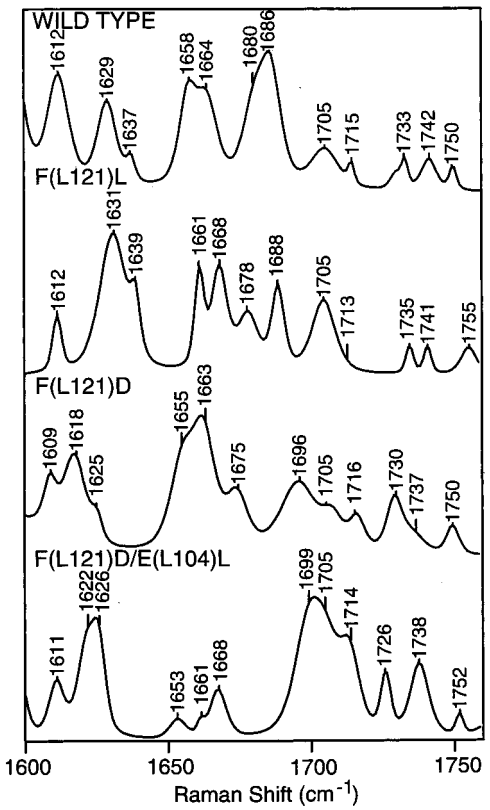

FIGURE 5: Comparison of the Q_y-excitation RR spectra of the BPhs of wild-type, F(L121)L, F(L121)D, and F(L121)D/E(L104)L RCs in the region of the carbonyl and high-frequency ring-skeletal modes. The spectra for wild-type and F(L121D) RCs are the same as the bottom traces of Figures 3 and 4.

siduals were obtained for the F(L121)L and F(L121)D/E(L104)L RCs (not shown). The reconstructed spectra for the wild-type and F(L121)D RCs are reproduced in Figure 5. The reconstructed spectra for the F(L121)L and F(L121)D/E(L104)L RCs are also included in Figure 5.

In addition to the spectra obtained with λ_{ex} = 760 nm (Figures 3−5), RR spectra were also obtained at other selected excitation wavelengths in the 750−770-nm region (not shown). These spectra do not reveal any additional features. Excitation in the 750−770-nm region in conjunction with observation in the high-frequency regime ensures that all of the observed RR bands are due to the two BPh cofactors (*26*). The 760-nm exciting line nominally falls closer to the absorption maximum of BPh_L; however, previous Q_y-excitation RR studies of RCs have shown that both BPh_L and BPh_M contribute to the high-frequency region of the RR spectrum with λ_{ex} = 760 nm (*26*).

Inspection of Figure 5 reveals that many of the general features of the RR spectra of the different genetically modified RCs are similar to one another and similar to those of wild-type RCs. For each of the RCs, the vibrations enhanced with Q_y excitation include the stretching modes of the C_{10a}-carbomethoxy (1725−1755 cm^{-1}), C_9-keto (1685−1705 cm^{-1}), and C_{2a}-acetyl (1650−1680 cm^{-1}) carbonyl groups as well as the stretching modes of the C_aC_m and unsaturated C_bC_b bonds (1600−1640 cm^{-1}) (*25*, *26*). The remaining stretching modes of the C_aC_m bonds as well as those of the C_aC_b and C_aN bonds occur at lower frequencies (1300−1600 cm^{-1}, not shown) (*25*,*26*).

The focus of the present study is on differences in the frequencies of analogous RR bands of BPh_L in the various RCs (and their positions relative to those of BPh_M) and not on differences in relative RR intensities. The frequencies of the RR bands are of particular interest because these features reflect the properties of the ground electronic states of the cofactors. In contrast, the RR intensities are strongly affected by the properties of the Q_y-excited states of the chromophores (via origin shifts and/or dephasing times of certain modes). These excited-state properties are outside the scope of this paper. Nonetheless, it should be noted that the RR intensity differences that are observed upon replacement of the native Phe L121 with Leu derive largely, if not exclusively, from electronic perturbations to the Q_y-excited state of BPh_L. This follows from the fact that the (ground-state) vibrational frequencies are virtually the same for wild-type and F(L121)L RCs (vida infra). The electronic ground-state absorption spectra of these two RCs are very similar as well (*9*). On the other hand, the replacement of Phe L121 with Asp causes the energy of the $Q_y(0,0)$ band of BPh_L to shift in both the F(L121)D and the F(L121)D/E(L104)L RCs relative to wild type. In the F(L121)D RCs, the $Q_y(0,0)$ band contour is split, and it is not clear whether the $Q_y(0,0)$ band of BPh_L is red- or blue-shifted (*18*). In the F(L121)D/E(L104)L RCs, the splitting of the band contour is larger, but the exact position of the $Q_y(0,0)$ band of BPh_L is still not certain (A. Cua and D. F. Bocian, unpublished results). For each of these mutants, the shift of the $Q_y(0,0)$ band of BPh_L, with respect to both the $Q_y(0,0)$ band of BPh_M and the 760-nm Raman exciting line, must also contribute to the intensity differences of certain RR bands of BPh_L relative to other bands of this cofactor and with respect to those of BPh_M. The fact that the RR frequencies of the BPh cofactors of the various genetically modified RCs are generally similar

Table 1: RR Frequencies (cm^{-1}) and Assignments[a] for the Carbonyl and Selected Ring-Skeletal Modes of BPh_L and BPh_M

	wild type		F(L121)L		F(L121)D		F(L121)D/E(L104)L	
description[b]	BPh_L	BPh_M	BPh_L	BPh_M	BPh_L	BPh_M	BPh_L	BPh_M
νC_{10a}═O	1733		1735		1730		1726	
	(1750, 1742)[c]		(1755, 1741)[c]		(1750, 1737)[c]		(1752, 1738)[c]	
combination(?)	1715		1713		1716		1714	
νC_9═O	1686	1705	1688	1705	1696	1705	1699	1705
νC_{2a}═O	1680		1678		1675		1668	
	(1664, 1658)[c]		(1668, 1661)[c]		(1663, 1655)[c]		(1661, 1653)[c]	
[νC_bC_b(III),$\nu C_aC_m(\gamma)$]	1637	1629	1639	1631	1618	1625	1622	1626
$\nu C_aC_m(\alpha,\beta,\gamma,\delta)$	1612[d]		1612[d]		1609[d]		1611[d]	

[a] Taken from ref *26*. [b] The designations C_a, C_b, C_m, III, α, β, γ, and δ refer to Figure 2. [c] The assignment of these two bands to BPh_L vs BPh_M is unclear (see text). [d] A single band is reported because these modes of BPh_L and BPh_M occur at the same frequency.

to one another and to those of wild-type RCs permits assignment of the vibrational modes of the mutants by direct analogy to those previously reported for wild-type RCs (*26*). The overall rationale for the vibrational assignments of the BPhs has been previously discussed in detail and will not be reiterated here. Although these earlier vibrational assignments were made for *Rb. sphaeroides* rather than *Rb. capsulatus* wild-type RCs (*26*), RR studies have shown that the spectral signatures of these two different wild-type RCs are quite similar (*36*, *37*). The frequencies and normal-mode descriptions of the principal RR bands observed in the 1600−1760-cm^{-1} region for the various RCs are summarized in Table 1. With the exception of a single RR band observed near 1715 cm^{-1} for all of the RCs, all of the observed bands are attributed to fundamental carbonyl or ring-skeletal stretching vibrations. The specific RR scattering characteristics of the various types of modes of the different RCs are discussed in more detail below.

Ring-Skeletal Modes. Two RR bands are observed above 1600 cm^{-1} that are due to ring-skeletal vibrations (Figure 5; Table 1). The highest frequency of these vibrations, [νC_bC_b-(III),$\nu C_aC_m(\gamma)$], is predominantly due to stretching of the unsaturated C_bC_b bond in ring III along with a smaller component involving stretching of the methine bridge in the ring III/V region of the cofactor (*26*, *38*). This mode has no analogue in metalloporphyrins and occurs at a relatively high frequency (<1615 cm^{-1}) owing to strain in the ring III/V region. In wild-type RCs, the [νC_bC_b(III),$\nu C_aC_m(\gamma)$] modes of BPh_L and BPh_M are not coincident and occur near 1637 and 1629 cm^{-1}, respectively (*26*). The F(L121)L mutation has a negligible affect on the frequency of the [νC_bC_b(III),$\nu C_aC_m(\gamma)$] mode of BPh_L (and that of BPh_M). This trend parallels that observed for the (absence of an) effect of the F(L121)L mutation on the frequencies of the carbonyl stretching modes (vide infra). On the other hand, Asp L121 has a dramatic effect on the frequency of the [νC_bC_b(III),$\nu C_aC_m(\gamma)$] mode of BPh_L. In the F(L121)D mutant, the [νC_bC_b(III),$\nu C_aC_m(\gamma)$] mode of BPh_L downshifts by nearly 20 cm^{-1} compared with wild type; in the F(L121)D/E(L104)L double mutant, the downshift is about 15 cm^{-1}. The large F(L121)D-induced shift that occurs in the frequency of the [νC_bC_b(III),$\nu C_aC_m(\gamma)$] mode for BPh_L parallels that observed for the νC_9═O vibration for this pigment (vide infra). Finally, it should be noted that small (≤4 cm^{-1}) shifts that appear to occur in the frequency of the [νC_bC_b(III),$\nu C_aC_m(\gamma)$] mode of BPh_M in the single and double mutants containing Asp L121 are probably due to uncertainties in the fitting procedures of the severely overlapped bands rather than actual differences.

The second ring-skeletal mode observed above 1600 cm^{-1}, $\nu C_aC_m(\alpha,\beta,\gamma,\delta,)$, is characterized by the stretching of all four methine bridges (*26*, *38*). This mode is the analogue of the ν_{10} vibration of metalloporphyrins and occurs near 1610 cm^{-1}. In wild-type RCs, the frequencies of the νC_aC_m-$(\alpha,\beta,\gamma,\delta)$ modes of BPh_L and BPh_M are coincident; thus, only a single band is observed in the RR spectrum (*23*−*26*) (Figure 5; Table 1). The *Rb. capsulatus* F(L121) and E(L104) mutations appear to have only a minor effect, if any, on the frequency of the $\nu C_aC_m(\alpha,\beta,\gamma,\delta)$ mode. The mutations also have relatively small (≤5 cm^{-1}) effects on the ring-skeletal modes in the 1300−1600-cm^{-1} region (not shown).

C_9-Keto Modes. The νC_9═O modes of BPh_L and BPh_M in *Rb. capsulatus* and *Rb. sphaeroides* wild-type RCs have been previously assigned and are observed at 1686 and 1705 cm^{-1}, respectively (*23*−*26*, *39*).[2] The νC_9═O mode of BPh_M is also observed at 1705 cm^{-1} for all three F(L121) mutants (Figure 5; Table 1). The F(L121)L mutation has a negligible effect on the frequency of the νC_9═O mode of BPh_L. In contrast, the F(L121)D and F(L121)D/E(L104)L mutations upshift the νC_9═O mode of BPh_L by 10 and 13 cm^{-1}, respectively. The small additional upshift observed for the double mutant is clearly apparent from the collapse of the SERDS band contour in the 1695−1705-cm^{-1} region from two distinct bands to a single band. The finding that the upshift observed upon introducing the E(L104)L mutation into the F(L121)D background is smaller than the 8-cm^{-1} upshift observed previously upon introducing the E(L104)L mutation into the wild-type background (*39*) suggests that the presence of Asp L121 weakens the hydrogen bond between the C_9-keto group of BPh_L and Glu L104.

C_{10a}-Carbomethoxy Modes. All four *Rb. capsulatus* RCs exhibit three RR bands in the region of the νC_{10a}═O modes. One of these bands occurs in the 1750−1755-cm^{-1} region, whereas the other two occur in the 1725−1745-cm^{-1} region (Figure 5; Table 1). Because two bands are nominally expected (if the frequencies for BPh_L and BPh_M are not coincident), the finding of three bands indicates the presence of populations of RCs having different environmental effects on the νC_{10a}═O mode(s) of at least one of the two BPhs. In

[2] Lutz and co-workers have reported the frequency of the νC_9═O mode of BPh_L as 1678 cm^{-1} (*23*−*25*). In our studies of RCs from a variety of species over a wide range of temperatures, the νC_9═O mode of BPh_L is always observed in the 1682−1686-cm^{-1} region (Table 1 and ref. *26*). The origin of this discrepancy is uncertain.

general, the frequency differences in these modes among the various RCs are relatively small (≤ 5 cm^{-1}), rendering assignment of the bands to BPh_L versus BPh_M ambiguous. The possible exception is the lowest frequency νC_{10a}=O mode, which is observed for wild-type at 1733 cm^{-1} and consistently downshifts in the F(L121)D and F(L121)D/E(L104)L mutants to 1730 and 1726 cm^{-1}, respectively. This trend suggests that this mode is a νC_{10a}=O vibration of BPh_L. The occurrence of a νC_{10a}=O band of BPh_L near 1730 cm^{-1} is consistent with the results of recent FT-IR studies on *Rb. sphaeroides* wild-type and E(L104)L mutant RCs (*40*).

C_{2a}-Acetyl Modes. All four *Rb. capsulatus* RCs exhibit at least three RR bands in the region of the νC_{2a}=O modes. These bands are spread throughout the 1650−1680-cm^{-1} region (Figure 5; Table 1). The occurrence of three bands indicates the existence of populations of RCs having different interactions between the C_{2a}-acetyl group and the protein or the macrocycle for at least one of the two BPhs. This situation parallels that observed for the νC_{10a}=O modes (vide supra). Owing to the occurrence of multiple bands, the severe overlap of the bands in this region, and the necessity to extract the band positions via fitting of the SERDS data, small (≤ 4 cm^{-1}) apparent frequency shifts of bands in the νC_{2a}=O mode among the RCs are not deemed meaningful. For the same reasons, assignment of the features in the 1650−1680-cm^{-1} region of the spectrum of each RC to BPh_L versus BPh_M is generally ambiguous. One exception is the highest-frequency mode, which undergoes a pronounced 7-cm^{-1} downshift from 1675 cm^{-1} in the F(L121)D single mutant to 1668 cm^{-1} in the F(L121)D/E(L104)L double mutant. The fact that this shift is elicited by the removal of the Glu L104 hydrogen bond to BPh_L strongly suggests that the highest-frequency band in the 1650−1680-cm^{-1} region for each of the four RCs is a νC_{2a}=O mode of BPh_L.

The above-noted observation and vibrational assignment confirm findings made previously on wild-type (*36*) and beta-mutant RCs (*41*) that removal of the hydrogen bond between Glu L104 and the C_9-keto group of BPh_L has consequences that extend beyond the site of direct interaction. In particular, the C_{2a}-acetyl group, which lies on the opposite side of the macrocycle from the C_9-keto group, is affected. The torsional potential of the νC_{2a}=O mode, which defines the angle of the C_{2a}-acetyl group with respect to the BPh_L ring, is apparently modulated by removal of the hydrogen bond to the C_9-keto group. This effect could occur either directly as a consequence of the change in π-electron distribution in the macrocycle or indirectly via repositioning of the cofactor in the protein pocket (*41*). Regardless, it should be noted that the observation of multiple νC_{2a}=O modes for one or both of the BPhs in all of the RCs implies that multiple torsional isomers of the C_{2a}-acetyl group exist independent of the presence of the hydrogen bond to Glu L104. Furthermore, these isomers do not necessarily arise from the effects of the protein matrix. Studies of metalloporphyrins in solution indicate that conjugating groups such as vinyl, formyl, and acetyl naturally exist in two nearly-equal-energy torsional conformations (*42*). These conformations are distinguished by whether the =CH_2 (vinyl) or =O (formyl and acetyl) fragment points predominantly toward the methine bridge or the adjacent β-pyrrole substituent. These considerations suggest that a relatively minor structural/electronic perturbation on BPh_L caused by removal of the hydrogen bond to the C_9-keto group could have detectable effects on the relative populations and frequencies of differing νC_{2a}=O modes of the chromophore. A similar situation exists for the C_{10a}-carbomethoxy group, which is even more closely electronically and structurally linked to the C_9-keto group (vide supra).

Other Modes. The single remaining band in the RR spectrum is observed near 1715 cm^{-1} and is relatively insensitive to the F(L121) mutations. On the basis of FT-IR studies of *Rb. sphaeroides* mutant and wild-type RCs, it has been suggested that bands in this spectral region could be due to νC_{10a}=O modes of BPh_L that are significantly downshifted by very strong hydrogen bonding interactions (*40*). However, the fact that the 1715-cm^{-1} band is insensitive to the incorporation of Asp L121 argues against this assignment. Alternatively, the 1715-cm^{-1} band may be a combination mode (*26*).

DISCUSSION

Replacement of Phe L121 with Asp has been shown previously to have a significant effect on the primary photochemistry (*18*). These changes in the rates and yields of electron transfer suggest that Asp L121 perturbs the reduction potential of BPh_L, thereby raising the free energy of $P^+BPh_L^-$. The RR studies reported herein were undertaken to elucidate how the vibrational characteristics and, hence, the structural/electronic properties of BPh_L are modified by mutations at residue L121. These properties of this cofactor in turn reflect the characteristics of the Asp L121 residue in F(L121)D-containing RCs that are central to how this residue perturbs the initial events of photoinduced charge separation. Two key questions concern the structure/conformation of BPh_L and the charge/protonation state of Asp L121. In the sections below, we address these issues in turn.

The first important finding that emerges from the studies of the mutants is that simply replacing the native aromatic Phe L121 residue with a nonaromatic amino acid such as Leu has no discernible effect on the vibrational characteristics and, hence, the physical/electronic ground-state structure of BPh_L. A corollary is that the native Phe L121 residue does not affect the electronic ground-state properties of the BPh_L macrocycle via multipole interactions involving the phenyl ring. These observations are consistent with the fact that the F(L121)L mutation does not alter the ground-state optical or photochemical properties of the RCs (*18*). On the other hand, the Phe L121 residue most likely does affect certain properties of the Q_y-excited-state BPh_L (as indicated by the difference in RR intensities for BPh_L in F(L121)L versus wild-type RCs).

The second important finding is that the introduction of Asp L121 causes significant frequency shifts in certain modes associated with BPh_L; however, these changes are localized in the ring III/V portion of the BPh_L macrocycle. This assessment is indicated by the fact that the νC_9=O and [νC_bC_b(III),$\nu C_aC_m(\gamma)$] modes are strongly perturbed by the incorporation of Asp L121, whereas more distant and global indicators of the cofactor's structure such as the νC_{2a}=O, $\nu C_aC_m(\alpha,\beta,\gamma,\delta)$, and other ring-skeletal modes are essentially unchanged (Table 1). These combined observations suggest that the incorporation of Asp L121 does not result in

significant structural/conformational changes in the BPh_L macrocycle. Instead, the perturbations localized in ring III/V must be an indirect consequence of purely electronic alterations of the π-system of the cofactor. Similarly, the perturbations of the primary photochemistry found in the F(L121)D mutant must ultimately derive from the effects of Asp L121 on the electronic/redox properties of BPh_L, including a shift in the free energy of $P^+BPh_L^-$.

The question that remains is the mechanism by which Asp L121 alters the electronic properties of BPh_L. Analysis of the pertinent vibrational data for BPh_L in the F(L121)D and F(L121)D/E(L104)L mutants leads to the assessment that the perturbation of the π-system of the cofactor mostly likely arises because Asp L121 is deprotonated and negatively charged. This assessment is based on the following considerations. If Asp L121 were instead protonated and neutral, the predominant interaction between the carboxyl group and the C_9-keto group of BPh_L would be dipole−dipole in nature. The dipole moment of the C_9-keto group lies along the carbon−oxygen bond vector, whereas that of the Asp-carboxyl lies approximately along a bisector of this group, regardless of the protonation/charge state of the Asp. This latter bond vector makes an angle of $>120°$ with respect to the carbon−oxygen bond vector of the C_9-keto group (*4*, *6*, *7*) (Figure 1, right panel). This angle is obtained under the reasonable assumption that the torsional conformation of the methylene group of Asp L121 is the same as that of the aromatic ring of the native Phe residue (Figure 1, left panel). Accordingly, the dipole moments of the two groups are quasi-antiparallel. Coupling between the quasi-antiparallel dipoles would nominally stabilize the charge-separated resonance form $C_9^+-O^-$, which makes a small contribution to the electronic structure of the C_9-keto group. The stabilization of the $C_9^+-O^-$ resonance form would serve to *lower* the frequency of the $\nu C_9{=}O$ vibration of BPh_L owing to slightly enhanced single-bond character. This effect is exactly opposite what is actually observed. In particular, the $\nu C_9{=}O$ mode of BPh_L for both the F(L121)D and the F(L121)D/E(L104)L RC is appreciably *upshifted* from that of wild type. Accordingly, the vibrational signature of the $\nu C_9{=}O$ mode is incompatible with dipole−dipole coupling being the predominant interaction between the C_9-keto group and the carboxyl of Asp L121. It should also be noted that the upshift of the $\nu C_9{=}O$ mode in RCs containing Asp L121 is incompatible with any type of additional hydrogen bonding to the C_9-keto group. Hydrogen bonding generally lowers the frequency of $\nu C{=}O$ modes (*22*−*26*, *39*). On the other hand, a relatively nonspecific charge−dipole interaction between the carboxyl group of a deprotonated, negatively charged Asp L121 and the C_9-keto group of BPh_L would tend to destabilize $C_9^+-O^-$ and all other charge-separated resonance forms. The destabilization of these resonance forms would tend to *upshift* the $\nu C_9{=}O$ mode owing to slightly enhanced double-bond character. This picture is entirely consistent with the experimental observations for both the F(L121)D and the F(L121)D/E(L104)L RC.

Additional support for a charge−dipole interaction between the Asp-carboxyl and C_9-keto groups can be found in the behavior of the $\nu C_9{=}O$ mode in the F(L121)D versus the F(L121)D/E(L104)L RC. In particular, the $\sim$3-cm^{-1} upshift of the $\nu C_9{=}O$ mode that results from removal of the hydrogen bond between Glu L104 and the C_9-keto group of BPh_L in the presence of Asp L121 (Table 1) is considerably smaller than the $\sim$8-cm^{-1} shift observed upon removal of the hydrogen bond in the absence of Asp L121 (*39*). These comparisons suggest that the F(L121)D mutation weakens the hydrogen bond between Glu L104 and the C_9-keto group of BPh_L. A diminished contribution of the $C_9^+-O^-$ resonance form to the electronic structure of the C_9-keto group owing to the presence of a neighboring charge would necessarily weaken interactions to the quasi-positively charged hydrogen of Glu L104. The large downshift observed for the $[\nu C_bC_b(III),\nu C_aC_m(\gamma)]$ mode in both the F(L121)D and the F(L121)D/E(L104)L RC could also be a direct consequence of interactions between a charged carboxyl group and the π-electronic system in the ring III/V region of BPh_L. However, any rearrangement of electron density in the C_9-keto group would necessarily also affect the electron density in the C_bC_b bond of ring III because these two double bonds are conjugatively adjacent to one another. The redistribution of electron density in both of these double bonds would have secondary consequences on the structure of the BPh_L macrocycle localized in the ring III/V region.

CONCLUSIONS

The vibrational characteristics of BPh_L in the mutant RCs containing Asp L121 strongly support a view in which the carboxyl group of this amino acid residue is deprotonated and negatively charged. These characteristics of BPh_L also suggest that the negatively charged carboxyl group of Asp L121 interacts with the π-electron system of the cofactor in a relatively nonspecific fashion, diminishing the contribution of charge-separated resonance forms of the C_9-keto group to the electronic structure of the macrocycle. The location of a negative charge near BPh_L is entirely consistent with the photochemistry of the Asp L121 RCs, which indicates that the free energy of $P^+BPh_L^-$ is significantly higher than that of the analogous charge-separated state of wild-type RCs (*18*).

REFERENCES

1. Deisenhofer, J., and Norris, J. R., Eds. (1993) *The Photosynthetic Reaction Center*, Vol. II, Academic Press, San Diego.
2. Blankenship, R. E., Madigan, M. T., and Bauer, C. E., Eds. (1995) *Anoxygenic Photosynthetic Bacteria*, pp 503−708, Kluwer Academic Publishers, Dordrect, The Netherlands.
3. Michel-Beyerle, M. E., Ed. (1996) *The Reaction Center of Photosynthetic Bacteria*, Springer, Berlin.
4. Ermler, U., Fritzsch, G., Buchanan, S., and Michel, H. (1994) *Structure 2*, 925−936.
5. Deisenhofer, J., Epp, O., Sinning, I., and Michel, H. (1995) *J. Mol. Biol. 246*, 429−457.
6. Yeates, T. O., Komiya, H., Chirino, A., Rees, D. C., Allen, J. P., and Feher, G. (1988) *Proc. Natl. Acad. Sci. U.S.A. 85*, 7993−7997.
7. El-Kabbani, O., Chang, C.-H., Tiede, D., Norris, J., and Schiffer, M. (1991) *Biochemistry 30*, 5361−5369.
8. Kirmaier, C., Gaul, D., DeBey, R., Holten, D., and Schenck, C. C. (1991) *Science 251*, 922−927.
9. Heller, B. A., Holten D., and Kirmaier, C. (1995) *Biochemistry 34*, 5294−5302.
10. Kirmaier, C., Laporte, L., Schenck, C. C., and Holten, D. (1995) *J. Phys. Chem. 99*, 8903−8909.
11. Kirmaier, C., Laporte, L., Schenck, C. C., and Holten, D. (1995) *J. Phys. Chem. 99*, 8910−8917.

12. Heller, B. A., Holten, D., and Kirmaier, C. (1995) *Science 269*, 940−945.
13. Scheer, H., and Gartwich, G. (1995) In *Anoxygenic Photosynthetic Bacteria* (Blankenship, R. E., Madigan, M. T., and Bauer, C. E., Ed.) pp (649-663, Kluwer Academic Publisher, Dordrecht, The Netherlands.
14. Shkurapatov, A. Y., and Shuvalov, V. A. (1993) *FEBS Lett. 322*, 168−172.
15. Schmidt, S., Arlt, T., Hamm, P., Huber, H., Nagele, T., Wachtveitl, J., Meyer, M., Scheer, H., and Zinth, W. (1994) *Chem. Phys. Lett. 223*, 116−120.
16. Huber, H., Meyer, M., Nagel, T., Hartl, I., Scheer, H., Zinth, and W., Wachtveitl, J. (1995) *Chem. Phys. 197*, 297−305.
17. Felton, R. H. (1978) In *The Porphyrins* (Dolphin, D., Ed.) Vol. V, pp 53−126, Academic Press, New York.
18. Heller, B. A., Holten D., and Kirmaier, C. (1996) *Biochemistry 35*, 15418−15427.
19. Bylina, E. J., Kirmaier, C., McDowell, L. M., Holten, D., and Youvan, D. C. (1988) *Nature 336*, 182−184.
20. Lin, X., Murchison, H. A., Nagarajan, V., Parson, W. W., Allen, J. P., and Williams, J. C. (1994) *Proc. Natl. Acad. Sci. U.S.A. 91*, 10265−10269.
21. Varadarajan, R., Zewert, T. E., Gray, H. B., and Boxer, S. G. (1989) *Science 243*, 69−72.
22. Lutz, M. (1984) *Adv. Infrared Raman Spectrosc. 11*, 211−300.
23. Lutz, M., and Robert, B. (1988) In *Biological Applications of Raman Spectroscopy* (Spiro, T. G., Ed.) Vol. 3, pp 347−411, Wiley, New York.
24. Lutz, M., and Mäntele, W. (1991) In *Chlorophylls* (Scheer, H., Ed.) pp 855−902, CRC Press, Boca Raton, FL.
25. Lutz, M. (1995) *Biospectroscopy 1*, 313−327.
26. Palaniappan, V., Martin, P. C., Chynwat, V., Frank, H. A., and Bocian, D. F. (1993) *J. Am. Chem. Soc. 115*, 12035−12049.
27. Palaniappan, V., Schenck, C. C., and Bocian, D. F. (1995) *J. Phys. Chem. 99*, 17049−17058.
28. Laporte, L. L., Palaniappan, V., Davis, D. G., Kirmaier, C., Schenck, C. C., Holten, D., and Bocian, D. F. (1996) *J. Phys. Chem. 44*, 17696−17707.
29. Czarnecki, K., Diers, J. R., Chynwat, V., Erickson, J. P., Frank, H. A., and Bocian, D. F. (1997) *J. Am. Chem. Soc. 119*, 415−426.
30. Czarnecki, K., Chynwat, V., Erickson, J. P., Frank, H. A., and Bocian, D. F. (1997) *J. Am. Chem. Soc. 119*, 2594−2595.
31. Cherepy, N. J., Shreve, A. P., Moore, L. J., Franzen, S., Boxer, S. G., and Mathies, R. A. (1994) *J. Phys. Chem. 98*, 6023−6029.
32. Cherepy, N. J., Holzwarth, A., and Mathies, R. A. (1995) *Biochemistry 34*, 5288−5293.
33. Cherepy, J. M., Shreve, A. P., Moore, L. J., Boxer, S. G., and Mathies, R. A. (1997) *Biochemistry 36*, 8559−8566.
34. Yu, N.-T., and Srivastava, R. B. (1980) *J. Raman Spectrosc. 9*, 166−171.
35. Shreve, A. P., Cherepy, N. J., and Mathies, R. A. (1992) *Appl. Spectrosc. 46*, 707−711.
36. Peloquin, J. M., Bylina, E. J., Youvan, D. C., and Bocian, D. F. (1990) *Biochemistry 29*, 8417−8424.
37. Palaniappan, V., and Bocian, D. F. (1995) *Biochemistry 34*, 11106−11116.
38. Donohoe, R. J., Frank, H. A., and Bocian, D. F. (1988) *Photochem. Photobiol. 48*, 531−537.
39. Palaniappan, V., and Bocian, D. F. (1995) *J. Am. Chem. Soc. 117*, 3647−3648.
40. Breton, J., Nabedryk, E., Allen, J. P., and Williams, J. C. (1997) *Biochemistry 36*, 4515−4525.
41. Czarnecki, K., Schenck, C. C., and Bocian, D. F. (1997) *Biochemistry 36*, 14697−14704.
42. Kalsbeck, W. A., Ghosh, A., Pandey, R. K., Smith, K. M., and Bocian, D. F. (1995) *J. Am. Chem. Soc. 117*, 10959−10968.

BI972410E